Adsorption of Pb(II) on a Composite Material Prepared from Polystyrene-Alumina and Activated Carbon: Kinetic and Thermodynamic Studies

R.A.K. Rao*, S. Ikram and J. Ahmad

Department of Applied Chemistry, Faculty of Engineering and Technology, Aligarh Muslim University, Aligarh 202002, Uttar Pradesh, India

The ability of polystyrene-alumina-activated carbon composite as a synthetic adsorbent was investigated for the removal of Pb(II) ions from aqueous solutions. Various physico-chemical parameters such as pH, initial metal ion concentration, adsorbent dosage and contact time were studied. The optimum solution pH for the maximum adsorption of Pb(II) was found to be 4. Kinetic data were best described by pseudo-second-order model. The adsorption process followed both Langmuir and Freundlich adsorption isotherms at 30 ℃. Thermodynamic studies indicated that the adsorption was spontaneous and endothermic in nature. Desorption studies were carried out by batch and column operations and it was found that 97% Pb(II) could be recovered by the column process using 0.1 M HCl as eluent.

INTRODUCTION

Safe handling, treatment and disposal of effluents containing heavy metals are of grave concern from the perspective of both health and environment [1]. Heavy metals pose serious threat to public health because of their non-biodegradable and persistent nature [2]. They are carcinogenic even at very low concentrations [3]. Major sources of heavy metal pollution are mining, welding, alloy manufacturing, tannery, jewelry, chemicals, fuel, ammunition and metallurgical, electrical and electronic goods producing industries in developed as well as developing countries [4].

A variety of conventional and modern methods have been devised for the effective removal of heavy metals from contaminated water. The most common are chemical precipitation, oxidation-reduction, electrochemical treatment,

*Corresponding author. E-mail: rakrao1@rediffmail.com

evaporative recovery, filtration, ion-exchange, solvent extraction, ultra filtration, reverse osmosis, electro dialysis, adsorption and membrane technologies [5-8]. However, most of these processes suffer from one drawback or the other, especially when the metals in solution are in the range of 1-100 mg l^{-1} [9]. For instance, precipitation methods are comparably simple and reliable but require high installation cost for setting large tanks for the effective precipitation. Moreover, there is a further need to treat the effluent in order to ensure that the treated water contains the impurities below the permissible limit.

Recently, adsorption technology has emerged as a powerful economical, simple and effective tool for the removal of heavy metal ions from wastewater [10]. Of all the known heavy metal ions, lead is a potential threat from the environmental point of view as, the metal is widely used in a variety of occasions particularly in lead smelting, battery manufacturing, paper and pulp industry and most importantly

in dentistry [11,12].

Lead combines with a variety of elements to form toxic compounds. The main target of lead toxicity is the central nervous system, apart from causing weakness in the fingers, wrists, and ankles. People with long-term lead exposure also complain of the increase in the blood pressure, particularly in middle-aged and elderly people, in addition to anemia. Prolonged exposure to lead can severely damage kidneys, liver, the central and peripheral nervous system, the reproductive system, *etc.* [13].

Keeping in mind the economic feasbility, simple mode of action and versatility of absorption process against a variety of heavy metal ions and organic dyes, a large number of absorbents like olyaniline modified clinoptilolite, polystyrene-bound pyridine, mesoporous carbon and saw dust have been used [14-17]. The significance of lead removal from water and wastewater by adsorption process can be appreciated by considering the fact that more than 2024 articles have been published on the removal of lead from aqueous solutions in the year 2009 alone.

These natural adsorbents are reasonably cheap and easily available, but they have their own limitations in that most of them do not yield reproducible results; therefore, synthetic adsorbents have been explored by many researchers. The advantage of synthetic adsorbents is that they can be produced on large scale with almost similar adsorption properties. Recently, many researchers have synthesized composite materials like dolomite powder, silica gel, zeolite/vermiculite, chemical modification of silica gel with diethylenetriamine, carbon natural zeolite, polyacrylamide-bentonite and zeolite, organically functionalized silica gel, multi-amine grafted mesoporous silicas, hydroxyapatite/polyacrylamide composite hydrogels, activated nylon-based membrane, activated carbon zeolite, magnetic zeolite, hydroxyapatite/polyurethane composite foams, and carbon nanotubes grown on micro-sized

Al_2O_3 particles, which possess better adsorption properties [18-31]. In the present work, a composite material was prepared by mixing polystyrene, alumina and small quantity of activated carbon at high temperature. Alumina and activated carbon are the most frequently studied adsorbents owing to their high adsorption capacity. Therefore, by mixing these two with polystyrene (binder), one may expect higher adsorption capacity. The adsorption properties of polystyrene-alumina-carbon (PAC) composite were explored and it was found that the composite shows strong affinity towards Pb(II) ions as compared to other such adsorbents.

EXPERIMENTAL

Preparation of the Adsorbent

The PAC composite is easy to synthesize. Polystyrene is a thermoplastic polymer that can be melted easily. Alumina (Al_2O_3) and activated carbon both possess high adsorption capacity. The dispersion of these two in the molten polystyrene which acts as a binder may produce a composite that should exhibit considerable adsorption properties. Polystyrene granules, alumina and activated carbon were mixed in different ratios. The mixture was transferred into a silica crucible and heated in a muffle furnace for 1 h with closed lid. The crucible was then taken out and cooled at room temperature. The solid material formed was taken out and named PAC. Sample No. P_3 (Table 1) was ground and then sieved to get 100-150 μm particle size. The sieved particles were then washed several times with double distilled water (DDW) and then dried in an oven at 60 °C.

Characterization of the Adsorbent

Scanning electron microscopy (SEM) analysis technique was employed to observe the surface morphology of the adsorbent. The types of binding groups present on the

Table 1. Synthesis of PAC

Sample	Polystyrene:Alumina:Carbon mixing ratio (g)	Heating temperature (°C)	Remark
P1	5:5:0.01	500	Hard and shiny
P2	5:1:0.10	500	Black, low density, soft powder
P3	5:5:0.10	500	Granular and porous mass

adsorbent were identified by Fourier transform infrared spectroscopy (FTIR). X-ray Diffraction (XRD) analysis was performed before and after adsorption.

Apparatus

The pH of the solution was measured with ELICO LI 120 pH-meter. A water bath incubator shaker model NSW-133, Narangs Scientific Work Private Limited, was used for shaking the adsorption batches. The concentration of the solutions before and after adsorption was measured by using GBC-902 Double Beam Atomic Absorption Spectrophotometer (AAS) (Australia). SEM analysis was done by LEO 435 VP model. FTIR analysis was done by using Perkin Elmer 1600 infrared spectrometer with pellets made of powdered KBr and adsorbent. XRD was done by using Bruker D8 Adv. GADDS instrument.

Adsorbate Solutions

All the chemicals used in the study were of analytical reagent grade and purchased from C.D.H. (Pvt.) Ltd., G.S. Chemicals Testing Lab, Allied Industry or S.D. Fine Chemical Ltd., India.

A stock solution of Pb(II) was prepared (1000 mg l^{-1}) by dissolving the required amount of $Pb(NO_3)_2$ in DDW and diluted to obtain the desired concentration ranging from 10-100 mg l^{-1}.

Adsorption Studies

Adsorption studies were carried out by the batch process. Known amount of adsorbent was placed in 250 ml conical flask containing 50 ml Pb(II) solution of known concentration and was shaken in a shaker for a given time period. The solutions was then filtered and the final concentration of Pb(II) was determined by AAS. The percentage adsorption and adsorption capacity were computed conventionally [32].

Determination of Point of Zero Charge

The zero surface charge characteristics of the adsorbent were determined using the solid addition method [33]. 50 ml of 0.1 M $NaNO_3$ solution was transferred into series of 100 ml stoppered conical flasks. The initial pH (pH_i) values of the solutions were roughly adjusted between 2 and 9 by adding either dilutes 0.1 M HCl or 0.1 M NaOH. The pH_i of these

solutions was then accurately noted. 0.5 g of the adsorbent was then added to each flask, and the flask was securely capped immediately. The suspension was manually shaken and allowed to equilibrate for 24 h with intermittent manual shaking. The final pH (pH_f) values of the supernatant liquid were noted. The difference between the initial and final pH ($\Delta pH = pH_i - pH_f$) was plotted against pH_i. The point of intersection of the resulting curve with the abscissa, at which $\Delta pH = 0$, gave the pH_{PZC}.

Effect of Adsorbent Dose

A series of 250 ml conical flasks each containing 50 ml of Pb(II) solution of 50 mg l^{-1} concentration were treated at 20 ℃ with varying amounts of the adsorbent (0.1, 0.2, 0.3, 0.4, 0.6, 0.8 and 1.0 g). The flasks were shaken in a shaker incubator and after equilibrium, the solutions were filtered. The amount of Pb(II) in the filtrate was then determined by AAS. The same procedure was repeated at 30, 40 and 50 ℃.

Breakthrough Volume

0.5 g of the adsorbent was put in a glass column (0.6 cm internal diameter) with glass wool support. 500 ml of Pb(II) solution of 50 mg l^{-1} initial concentration (C°) was then passed through the column with a flow rate of 1 ml min^{-1}. The effluent was collected initially in 10 ml and then 50 ml fractions and the amount of Pb(II) was then determined in each fraction with the help of AAS. The breakthrough curve was obtained by plotting C/C° versus bed volume of the effluent.

Desorption Studies

Desorption studies were carried out by the batch as well as column process. In batch process, desorption of Pb(II) was carried out by treating 0.5 g of the adsorbent with 50 ml of Pb(II) solution (50 mg l^{-1}) in a conical flask. The solution was filtered after 24 h. The adsorbent was then washed several times with DDW to remove any excess of Pb(II). It was then treated with 50 ml of 0.1 M HCl solution and then filtered after 24 h. The filtrate was analyzed for Pb(II) desorbed. The same procedure was repeated with sodium chloride, acetic acid, sodium sulphate, sodium hydroxide and EDTA solutions.

Desorption studies by column process were carried out as follows. The exhausted column (from breakthrough capacity)

933

was washed several times with DDW to remove excess of Pb(II) ions from the column, then 0.1 M HCl was passed through the column containing adsorbed Pb(II). The eluted Pb(II) ions were collected in 10 ml fractions. The flow rate was maintained at 1 ml min^{-1}.

RESULTS AND DISCUSSION

Selectivity Study

The preliminary adsorption study was done on Pb(II), Cd(II), Cr(VI), Cu(II) and Ni(II). The percent sorption behavior of different metal ions on PAC was found to be Pb(II) 78%, Cd(II) 74%, Cr(VI) 48%, Cu(II) 46% and Ni(II) 44%. The initial selectivity results showed that the adsorption of Pb(II) was the maximum (figure not shown). Therefore, Pb(II) was selected as a model adsorbate to study the potential adsorbent PAC.

Adsorbent Characteristics

The details of the adsorbent prepared by mixing polystyrene, alumina and activated carbon in different ratios are reported in Table 1. Sample P_1 was hard and shiny and not easily ground. Sample P_2 was of a low density, black soft powder floating on the water surface on physical examination. Therefore, samples P_1 and P_2 were unsuitable for adsorption studies. Sample P_3 was granular mass and chosen for further studies.

Figure 1A is the SEM image of the native sample (P3) showing minute spots which could be due to the dispersion of very small quantity of the activated carbon on the polystyrene-alumina composite. Figure 1B is the image of sample after Pb(II) adsorption which shows distinct morphology from the native PAC. However, adsorption was not uniform as indicated by the bright and dull white patches. It is well documented in the literature that activated carbon has higher adsorption capacity as compared to its non-activated analogue [34-36]. The higher adsorption capacity of the activated carbon may be regarded to be due to the presence of micropores and ultra micropores yielding large surface area up to 2000 cm^2 g^{-1}. In this study, activated charcoal was used which shows maximum adsorption capacity. XRD before and after adsorption shows similar peaks (Figs. 2a and 2b) indicating that the adsorbent is a crystalline in nature.
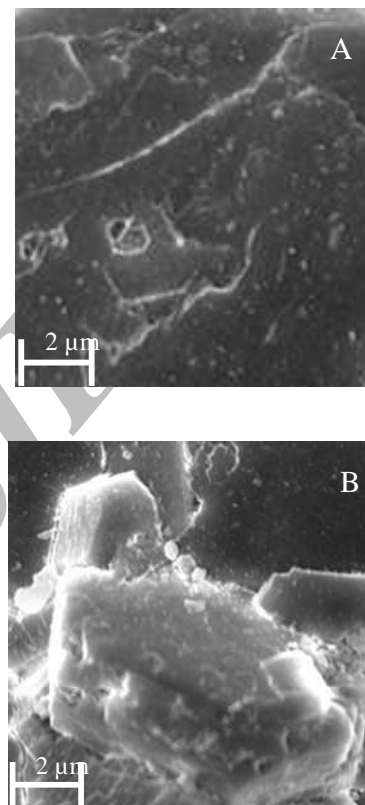

Fig. 1. SEM images of PAC: (A) before adsorption; (B) after Pb(II) adsorption.

FTIR Spectroscopy

Figure 3a shows peaks at 2923-3393 cm^{-1} which represent the C-H bonds of aromatic hydrocarbon (polystyrene). The peak at 1729 cm^{-1} represents the ketone group and at 1632 cm^{-1} indicates the aromatic C=C bonds (benzene ring in polystyrene) while the peak at 1462 cm^{-1} is characteristic of aromatic compounds [39]. Another peak at 1058 cm^{-1} may be due to stretching vibration of Al-O groups. Figure 3b represents the FTIR spectrum of PAC after Pb(II) adsorption from aqueous solution. These broad peaks at 3430 and 3362 cm^{-1} are due to H_2O and OH stretching vibrations respectively, after the adsorption of water molecules. The peak at 1058 cm^{-1} is reduced to 1029 cm^{-1} and broadened due to the adsorption of Pb(II) at Al-O groups while the peak at 1729 cm^{-1} represents the presence of the acetone group. FTIR spectra of alumina, the activated carbon and polystyrene show prominent peaks at 2900, 1450, 1400, 620, 550, 3400, 2900, 1650 and 3100, 3000,
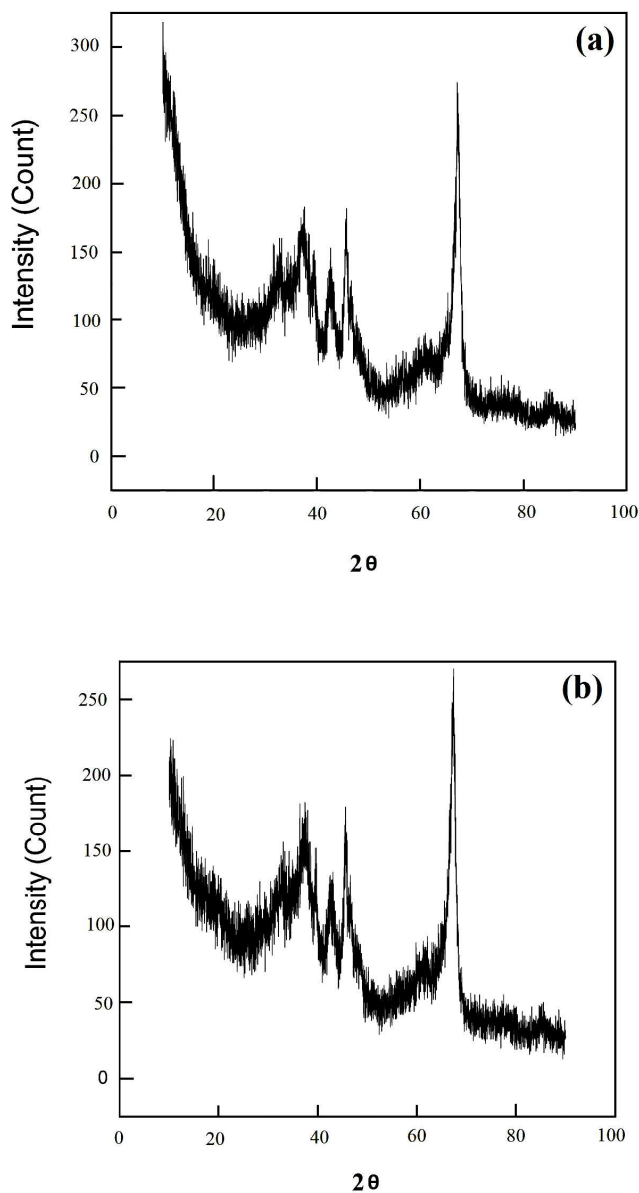
Fig. 2. XRD of PAC: (a) before adsorption; (b) after Pb(II) adsorption.

2900, 1650, 1500, 620 cm^{-1} [38-40] which are also seen in the PAC signifying the presence of these compounds in the adsorbent.

Effect of Contact Time and Initial Pb(II) Ion Concentration

A series of 250 ml conical flasks, each having 0.5 g adsorbent and 50 ml solution of known Pb(II) concentration, were shaken in a shaker incubator and at the pre-determined intervals. The solution of the specified flask was taken out and filtered. The concentration of Pb(II) in the filtrate was determined by AAS.

The effect of Pb(II) concentration in the solution for five different concentrations of Pb(II) (10, 20, 50, 80 and 100 mg
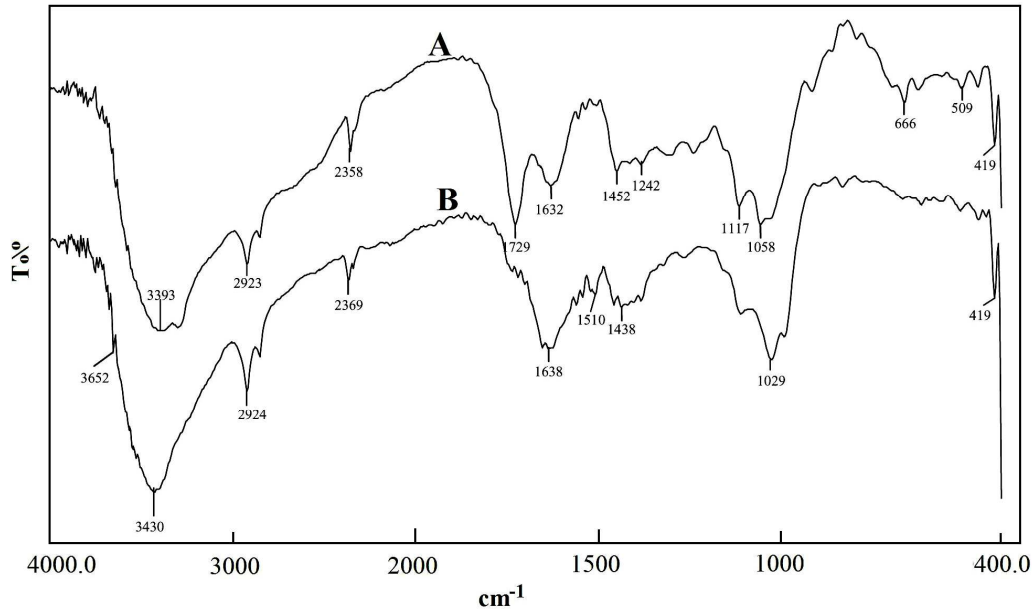
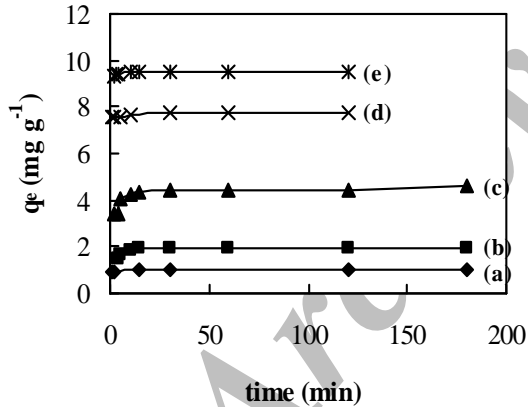**Fig. 3.** FTIR spectra of PAC: (A) before adsorption; (B) after Pb(II) adsorption.

Fig. 4. Effect of contact time on the adsorption of Pb(II) on PAC at various initial concentrations. (a) 10 mg l^{-1}, (b) 20 mg l^{-1}, (c) 50 mg l^{-1}, (d) 80 mg l^{-1}, (e) 100 mg l^{-1}.

l^{-1}) is shown in Fig. 4. It can be seen that the adsorption capacity (q_e) increases with an increase in the initial Pb(II) concentration. The adsorption capacity increases with time in the said concentrations, and after 10 min, it becomes independent of time (Fig. 4). The adsorption capacities at 10, 20, 50, 80 and 100 mg l^{-1} concentration were found to be 0.97,

1.94, 4.4, 7.8 and 9.51 mg g^{-1}, respectively.

Effect of pH

The effect of pH on the adsorption of Pb(II) was studied as follows: 100 ml of 50 mg l^{-1} Pb(II) solution poured into a beaker. The pH of the solution was adjusted between 2 and 9 by adding either dilute HCl or NaOH solution. 50 ml of this solution poured into a conical flask and treated with 0.5 g of the adsorbent and after equilibrium, the final concentration of Pb(II) was determined. The effect of pH on percent adsorption of Pb(II) is shown in Fig. 5. Pb(II) uptake increases with an increase in pH reaching to a maximum (90%) at pH ≥ 4. At initial pH 2, the adsorption is minimum (50%) and at final pH or pH_f (at equilibrium) is slightly increased (pH_f = 3.2). When pH_i is increased to 4, pH_f increases sharply (pH_f = 7) and, at the same time, adsorption of Pb(II) increases to maximum (90%). However, when pH_i is further increased, there is no significant increase in the %adsorption and pH_f increases very little.

The variation of %adsorption with respect to pH can be explained on the basis of the surface charge on the adsorbent and speciation of Pb(II). At pH 2, the negatively charged surface is protonated due to the presence of excess H^+ ions
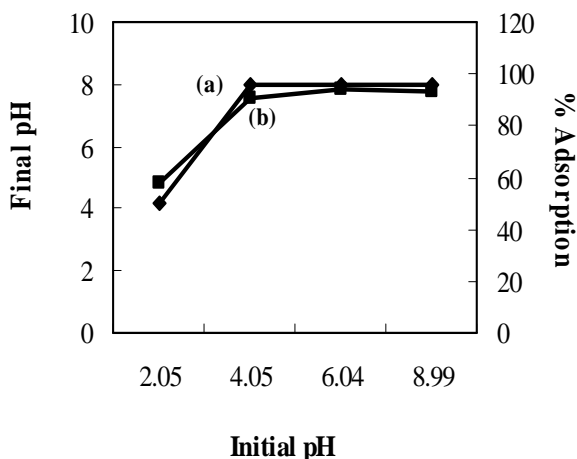
936

Fig. 5. Effect of the solution pH on the adsorption of Pb (II) on PAC. Conditions: (a) final pH, (b) %adsorption, $C_0 = 50$ mg l^{-1}, adsorbent = 0.5 g, T = 30 °C.
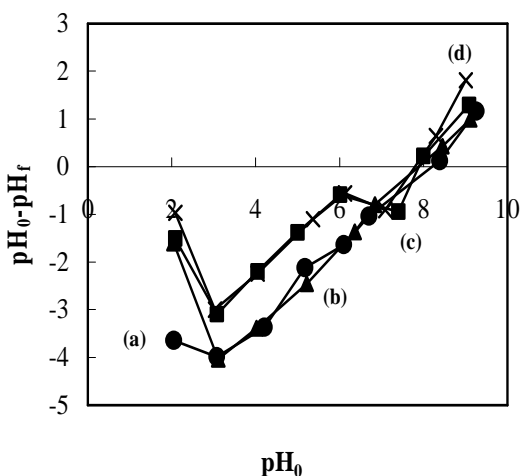

Fig. 6. Point of zero charge of PAC by solid addition method in presence of (a) DDW, (b) Pb(II) (DDW), (c) 0.1 M NaNO$_3$, (d) Pb(II) (0.1 M NaNO$_3$).

which does not favor Pb(II) ions adsorption due to electrostatic repulsion. When pH of the solution is increased, different species of Pb(II) are formed like Pb^{2+} (pH 1-6), Pb(OH)$^+$ (pH 7-8) and Pb(OH)$_2$ (pH 9-12) [41]. Therefore, when pH of the solution is increased to above 2, some of the

adsorption sites are deprotonated and Pb^{2+} ions are adsorbed along with H$^+$ ions, hence the equilibrium pH (pH$_f$) increases to 3.2. When initial pH is adjusted to 4, more and more Pb^{2+} ions are adsorbed along with some H$^+$ ions and pH$_f$ increases to 7. Since in the pH range 1-6, Pb^{2+} are predominant species, it can be concluded that the maximum adsorption of Pb(II) occurs in the form of Pb^{2+} up to pH 4. The solution pH also influences the surface charge of the adsorbent. The surface of the adsorbent is positive at pH < point of zero charge (pH$_{Pzc}$), neutral at pH = pH$_{Pzc}$ and negative at pH > pH$_{Pzc}$. The pH$_{Pzc}$ of the adsorbent is 8.2 when the adsorbent is treated with DDW (Fig. 6) and shifts towards lower pH value with an increase in electrolyte (NaNO$_3$) concentration as well as in the presence of Pb(II) ions indicating specific adsorption of counter ions [42].

Adsorption Isotherm

The Pb(II) ion uptake capacity of the adsorbent was evaluated using the Langmuir and Freundlich adsorption isotherms. Langmuir model is commonly used for liquid phase adsorption which assumes that the uptake of metal ions occurs on a homogeneous surface by monolayer adsorption without any interaction between adsorbed ions. The Langmuir isotherm is expressed as follows [43].

$$1/q_e = 1/q_m \times b \times 1/c_e + 1/q_m \tag{1}$$

where, q_e is the amount of Pb(II) adsorbed per unit weight of the adsorbent (mg g^{-1}) at equilibrium, C_e is the equilibrium concentration (mg l^{-1}), b and q_m are Langmuir constants related to the energy of adsorption (l mg^{-1}) and monolayer adsorption capacity of the adsorbent (mg g^{-1}), respectively. The linear plot of $1/q_e$ *vs.* $1/C_e$ (figure not shown) shows that adsorption of Pb(II) follows the Langmuir model. The values of q_m and b were calculated from the intercept and slope of the plots. The Freundlich isotherm is represented by the following equation [44].

$$\log q_e = \log K_f + 1/n \log C_e \tag{2}$$

where, C_e is the equilibrium concentration (mg l^{-1}), q_e is the amount adsorbed per unit weight of the adsorbent (mg g^{-1}) at equilibrium, K_f and n are constants designating adsorption capacity and adsorption intensity, respectively. Linear plots of

937

www.SID.ir

Table 2. Langmuir Parameters at Different Temperatures for the Adsorption of Pb(II) on PAC

Temperature (°C)	b (1 mg^{-1})	q_m (mg g^{-1})	RL	χ^2	R²
20	0.230	10.64	0.08	0.73	0.8954
30	0.790	22.47	0.02	0.43	0.9972
40	0.110	09.90	0.15	2.06	0.8976
50	0.049	16.72	0.29	0.70	0.8093

Table 3. Freundlich Parameters at Different Temperatures for the Adsorption of Pb(II) on PAC

Temperature (°C)	K_f	n	χ^2	R²
20	2.43	1.9	0.51	0.8592
30	7.76	1.8	0.02	0.9989
40	1.30	1.7	0.13	0.8988
50	1.30	1.7	0.59	0.6994

$\log q_e$ *vs*. $\log C_e$ (figure not shown) show that the adsorption followed Freundlich model. The values of K_f and n were calculated from the intercept and slope of the plots. According to Kadirvelu and Namasivayam [45], 'n' values lying between 1 and 10 represent the beneficial adsorption. The Langmuir and Freundlich parameters calculated at different temperatures are reported in Tables 2 and 3. A chi-square (χ^2) test was also run on these models.

$$\chi^2 = \sum (q_e\,(exp) - q_e\,(cal))^2/q_e\,(cal) \tag{3}$$

where q_e(exp) is the value obtained from the experiment and q_e(cal) is the value calculated from the model. If the data from the model are similar to the experimental data, χ^2 would be small and vice versa. It can be inferred from Tables 2 and 3 that both Langmuir and Freundlich isotherm models function best at 30 °C as it is evident from the low values of χ^2 and high values of coefficient of regression (R^2). The essential characteristic of Langmuir isotherm can be expressed in terms of dimensionless constant separation factor or equilibrium parameters (R$_L$) [46] which is given as

$$R_L = 1/b + C^o \tag{4}$$

where C^o is the initial Pb(II) concentration (mg l^{-1}) and b is Langmuir constant. R$_L$ values predict the slope of the isotherm. If R$_L$ > 1, then adsorption is unfavorable; if R$_L$ = 1, linear and 0 < R$_L$ <1, adsorption is favorable; and if R$_L$ = 0, adsorption is irreversible. The R$_L$ values (Table 2) obtained in the present case are less than 1 at all temperatures signifying favorable adsorption.

Table 4 summarizes the monolayer sorption capacities (q$_m$) of various synthetic adsorbents suggested prior to this study [2,13,47-49]. PAC exhibits higher sorption capacity implying a promising future for PAC utilization in Pb(II) ions removal from aqueous solutions.

Thermodynamic Studies

The variation in the extent of adsorption with respect to temperature has been explained based on the thermodynamic parameters *viz.* changes in standard free energy, enthalpy and entropy. The dependence on temperature of adsorption of Pb(II) on the adsorbent was evaluated using van't Hoff equation which is given as

$$\log K_c = - (\Delta H^o/2.303) \times (1/RT) + (\Delta S^o/2.303) \times 1/R \tag{5}$$

K$_c$ is the equilibrium constant that can be calculated as

938

Table 4. Comparison of Maximum Monolayer Sorption Capacity of Various Adsorbents for Pb(II) Removal

Adsorbent	q_m (mg g^{-1})	Ref.
Modified kaolinite clay	20.00	[2]
Acid activated and manganese oxide-coated bentonite	8.92	[13]
Hazelnut husk (activated carbon)	13.05	[47]
Bagasse flyash	2.50	[48]
Activated carbon	2.95	[49]
PAC	22.47	Present study

Table 5. ThermoDynamics Parameters

Temperature (°C)	lnKc	$\Delta G°$ (kJ mol^{-1})	$\Delta H°$ (kJ mol^{-1})	$\Delta S°$ (kJ mol^{-1} K^{-1})
20	0.94	-2.3	55.91	0.19
30	1.88	-4.7		
40	2.03	-5.3		
50	3.13	-8.4		

$$K_c = CA_c/C_e \qquad (6)$$

where CA_c is the amount of Pb(II) on the adsorbent (mg l^{-1})

and C_e is the amount of Pb(II) in the solution (mg l^{-1}) at equilibrium. The free energy change ($\Delta G°$) can be calculated from the following relation.

$$\Delta G° = -RT \ln K_c \qquad (7)$$

From the slope and intercept of the linear plot of $\ln K_c$ *vs*. 1/T (figure not shown), the values of $\Delta H°$ and $\Delta S°$ were computed. The values of these parameters are reported in Table 5. The overall free energy change during the adsorption process at all temperatures was negative, corresponding to a spontaneous process. The positive value of enthalpy change ($\Delta H° = +55.91$ kJ mol^{-1}) indicates that the adsorption process is endothermic [50]. The positive entropy change ($\Delta S°$) (+0.19 kJ mol^{-1} K^{-1}) indicates increase in randomness at the solid liquid interface. The above results show that adsorption process is enthalpy driven.

Adsorption Kinetics

In order to investigate the mechanism of adsorption and the potential rate-controlling steps, such as mass transport and chemical reactions, kinetic models were used to testify the experimental data. The pseudo-first-order model derived by Lagergren [51] has found wide applications. The pseudo-first-order model is expressed as

$$\log(q_e - q_t) = -K_1/2.303 \times t + \log q_e \qquad (8)$$

where, q_e (mg g^{-1}) and q_t are the amounts of adsorbed metal ions at equilibrium and at any time (t), respectively. K_1 (min^{-1}) is the pseudo-first-order adsorption rate constant. q_e and K_1 can be calculated from the slope and intercept of the plots of $\log(q_e - q_t)$ versus t (figure not shown). The values of K_1 and q_e calculated from the model indicated that this model had failed, since the experimental values of q_e differed appreciably from q_e calculated from the model (Table 6). Several authors [52-54] have shown that pseudo-second-order kinetic model can adequately describe these interactions in certain specific cases. The pseudo-second-order model is based on the assumption

939

Table 6. Pseudo-First-Order and Pseudo-Second-Order Kinetics Parameters

Concentration (C°) (mg l^{-1})	Pseudo-first-order				Pseudo-second-order			
	q_e (experimental) (mg g^{-1})	q_e (Calculated) (mg g^{-1})	K_1	R^2	q_e (Calculated) (mg g^{-1})	h	K_2	R^2
10	0.97	0.087	1.079	0.9996	0.97	38.30	40.70	1.0000
20	1.94	0.380	0.038	0.1793	2.13	01.50	00.33	0.9990
50	4.40	1.200	0.170	0.8071	4.57	03.35	00.16	0.9993
80	7.80	0.250	0.010	0.7503	7.80	24.60	00.40	1.0000
100	9.51	0.210	0.130	0.9372	9.50	172.40	01.90	1.0000

that adsorption follows a second order mechanism. So, the rate of occupation of adsorption sites is proportional to the square of the number of unoccupied sites.

The second-order model is expressed as

$$t/q_t = 1/h + 1/q_t \times t \qquad (9)$$

where, h is the initial adsorption rate which is equal to $K_2 \times q_e^2$, K_2 is the pseudo-second- order adsorption rate constant (g mg^{-1} min^{-1}). The q_e and K_2 can be calculated from the slope and intercept of the plot t/q_t *vs*. t (Fig. 7). The correlation coefficient (R^2) for the pseudo-second-order kinetic model was 1.0000 and the calculated values of q_e also agreed with the experimental values. Both factors suggest that the adsorption of Pb(II) ions followed pseudo-second-order kinetic model, indicating that the rate limiting step was a chemical adsorption process. Similar conclusions were reached by Ho and Mckay [55] who reported that most of the adsorption systems follow pseudo-second-order kinetic model. The values of regression coefficients, rate constants of pseudo-first-order model and pseudo-second-order parameters are reported in Table 6.

Intra-Particle Diffusion

The rate constant for intra-particle diffusion (K_{id}) is calculated by the equation [56]

$$q_t = K_{id} \times t^{1/2} + I \qquad (10)$$

where, q_t is the amount adsorbed (mg g^{-1}) at time t (min). Plots of q_t *vs*. $t^{1/2}$ are shown in Fig. 8 for different concentrations.
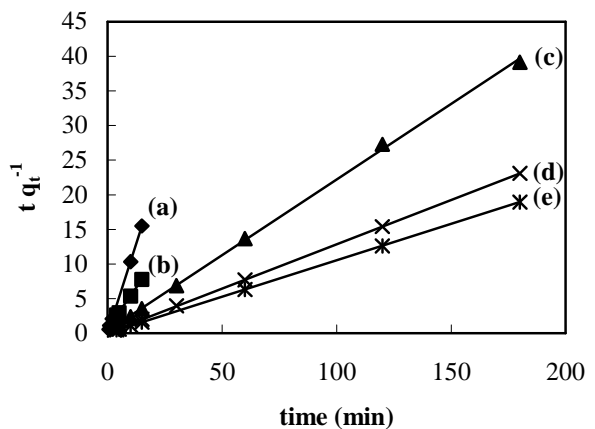

Fig. 7. Pseudo-second order kinetics for the adsorption of Pb(II) at various initial concentrations.(a) 10 mg l^{-1}, (b) 20 mg l^{-1}, (c) 50 mg l^{-1}, (d) 80 mg l^{-1}, (e) 100 mg l^{-1}.

The deviation in the plots from the origin for all concentrations indicate that pore diffusion is not the only rate limiting step, rather, some other processes like film diffusion, *etc.*, are also involved in the adsorption process.

Breakthrough Volume

Breakthrough curves are important in process design because they directly affect the feasibility and economics of the process. Figure 9 shows that 5 bed volumes (corresponding to 0.5 mg Pb(II)) could be passed through the column without detecting Pb(II) in the effluent when 0.5 g adsorbent was used.
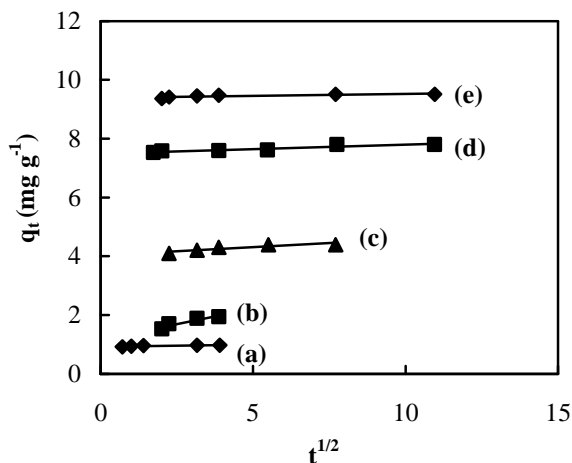
940

Fig. 8. Intra-particle diffusion plot for the adsorption of Pb(II) on PAC at various initial concentrations. (a) 10 mg l^{-1}, (b) 20 mg l^{-1}, (c) 50 mg l^{-1}, (d) 80 mg l^{-1}, (e) 100 mg l^{-1}.

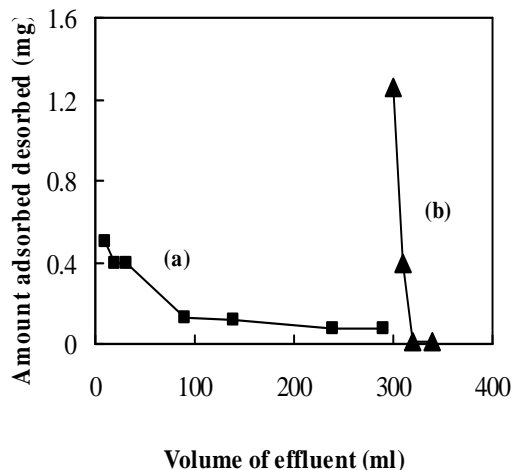**Fig. 9.** Breakthrough volume for the adsorption of Pb(II) on PAC.

Fig. 10. Adsorption and desorption of Pb(II) through column process. Conditions: (a) Pb(II) adsorbed (mg), (b) Pb(II) desorbed (mg), Co = 50 mg l^{-1}, adsorbent = 0.5 g, Flow rate = 1 ml min^{-1}, eluent = 0.1 M HCl.
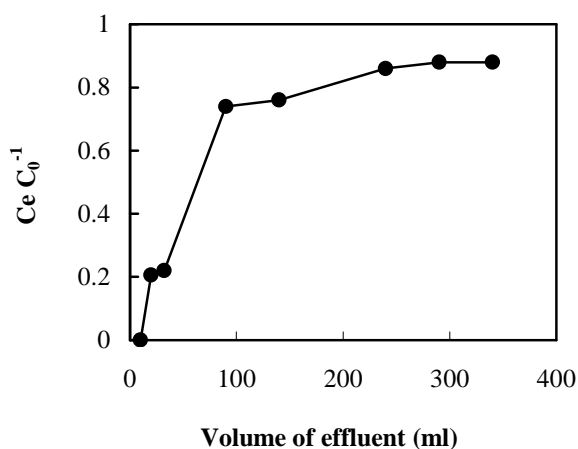
The sorbent capacity was found to be 2.34 mg g^{-1}.

Desorption Studies

Desorption studies were carried out by batch as well as by column process. Table 7 shows desorption of Pb(II) by various solvents eluting agents using batch process. Pb(II) is strongly adsorbed and could not be recovered by Na$_2$SO$_4$, NaCl or CH$_3$COOH solutions. However, 50% of Pb(II) could be recovered using 0.1 M HCl or 0.1 M EDTA solutions. Pb(II) can also be recovered to some extent (38%) with 0.1 M NaOH, perhaps due to the formation of Pb(OH)$_2$. However, excellent results were obtained when desorption studies were carried out by the column process.

Figure 10 shows that 1.67 mg Pb(II) is retained when 290

Table 7. Desorption of Pb(II) from PAC by Batch Process

Solvents	Amount loaded (mg)	Amount adsorbed (mg)	Amount recovered (mg)	Recovery (%)
0.1 M HCl	2.50	2.50	1.25	50
0.1 M NaCl	2.50	2.50	0.05	2
0.1 M Na$_2$SO$_4$	2.50	2.50	0.05	2
0.1 M NaOH	2.50	2.50	0.95	38
0.1 M CH$_3$COOH	2.50	2.50	0.05	2
0.1 M EDTA	2.50	2.50	1.25	50

ml of Pb(II) solution (50 mg l^{-1}) was passed through the column. The adsorbed Pb(II) was then eluted with 0.1 M HCl solution. It is important to note that the desorption of Pb(II) is rapid and the maximum amount of Pb(II) could be recovered within the first 10 ml fraction (1.53 mg). A total of 1.63 mg of Pb(II), corresponding to 97%, could be recovered within 40 ml of the effluent. In the batch process, the desorption or recovery is always less because the adsorbent is in contact with a fixed volume of the solution, hence an equilibrium, after certain amount of time, between the desorbed Pb(II) ions in the solution and the adsorbed Pb(II) ions in the adsorbent phase. This is not the case in the continuous flow column operation. Equilibrium is not established between the dynamic flow of the eluent and the adsorbent hence more and more Pb(II) ions are released from the adsorbent during the desorption process resulting in high recovery.

CONCLUSIONS

PAC composite was synthesized under various mixing ratios and its adsorption properties were explored. The adsorption of various heavy metals followed the order: Pb(II) > Cd(II) > Cr(VI) > Cu(II) > Ni(II). The ability of PAC to adsorb Pb(II) from water was studied in detail. The extent of the removal depended upon concentration, pH and temperature and contact time. The adsorption process followed both Langmuir and Freundlich adsorption isotherms at 30 ºC. The process was endothermic in nature and followed pseudo-second-order kinetics model. Desorption studies were carried out by batch and column operation using various eluents. Excellent results were obtained when Pb(II) was desorbed by 0.1 M HCl using column process and 97% Pb(II) was recovered.

ACKNOWLEDGMENTS

REFERENCES

[1]   J.O. Nriagu, J.M. Pacyna, Nature 333 (1988) 134.

[2]   M. Jiang, Q. Wang, X. Jin, Z. Chen, J. Hazard. Mater. 170 (2009) 332.

[3]   X. Bosch, Science 609 (2003) 1.

[4]   M. McCann, Am. J. Ind. Med. 30 (1996) 125.

[5]   N. Unlu, M. Ersoz, J. Hazard. Mater. 136 (2006) 272.

[6]   S.E. Bailey, T.J. Olin, R.M. Bricka, D.D. Adrian, Water Res. 33 (1999) 2469.

[7]   S.V. Joshi, S.H. Mehta, A.P. Rao, A.V. Rao, Water Treat. 7 (1992) 207.

[8]   K.C. Sekhar, S. Subramanian, J.M. Modak, K.A. Natarajan, Int. J. Miner. Process 53 (1998) 107.

[9]   S.S. Ahluwalia, D. Goyal, Bioresour. Technol. 98 (2007) 2243.

[10]   O. Moradi, M. Aghaie, K. Zare, M. Monajjemi, H. Aghaie, J. Hazard. Mater. 170 (2009) 673.

[11]   S.S. Gupta, K.G. Bhattacharyya, J. Environ. Manage. 87 (2008) 46.

[12]   D.F.C. Guedes, R.S. Silva, M.A.M.S. da Veiga, J.D. Pecora, J. Hazard. Mater. 170 (2009) 855.

[13]   E. Eren, B. Afsin, Y. Onal, J. Hazard. Mater. 161 (2009) 677.

[14]   A. Olad, M. Khatamian, B. Naseri, J. Iran. Chem. Soc. 8 (2011) S141.

[15]   M.R. Iravani, S. Tangestaninejad, M.H. Habibi, V. Mirkhani, J. Iran. Chem. Soc. 7 (2010) 791.

[16]   M. Anbia, A. Ghaffari, J. Iran. Chem. Soc. 8 (2011) S67.

[17]   R. Ansari, Z. Mosayebzadeh, J. Iran. Chem. Soc. 7 (2010) 339.

[18]   E. Pehlivan, A.M. Özkan, S. Dinç, Ş. Parlayici, J. Hazard. Mater. 167 (2009) 1044.

[19]   F. An, B. Gao, Desalination 249 (2009) 1390.

[20]   C.D. Johnson, F. Worall, Water Res. 41 (2007) 2229.

[21]   Y. Zhang, R. Qu, C. Sun, C. Wang, C. Ji, H. Chen, P. Yin, Appl. Surf. Sci. 255 (2009) 5818.

[22]   P.R. Shukla, S.B. Wang, H.M. Ang, M.O. Tadé, Adv. Powder Technol. 20 (2009) 245.

[23]   U. Ulusoy, S. Simsek, J. Hazard. Mater. B127 (2005) 163.

[24]   H. Wang, J. Kang, H. Liu, J. Qu, J. Environ. Sci. 21 (2009) 1473.

[25]   L. Zhang, C. Yu, W. Zhao, Z. Hua, H. Chen, L. Li, J. Shi, J. Non-Cryst. Solids 353 (2007) 4055.

[26]   S.H. Jang, Y.G. Jeong, B.G. Min, W.S. Lyoo, S.C. Lee,

J. Hazard. Mater. 159 (2008) 294.

[27] Z.Y. He, H.L. Nie, C.B. White, L.M. Zhu, Y.T. Zhou, Y. Zheng, Bioresour. Technol. 99 (2008) 7954.

[28] V.K. Jha, M. Matsuda, M. Miyake, J. Hazard. Mater. 160 (2008)148.

[29] L.C.A. Oliveira, D.I. Petkowicz, A. Smaniotto, S.B.C. Pergher, Water Res. 38 (2004) 3699.

[30] S.H. Jang, B.G. Min, Y.G. Jeong, W.S. Lyoo, S.C. Lee, J. Hazard. Mater.152 (2008) 1285.

[31] S.H. Hsieh, J.J. Horng, J. Univ. Sci. Technol. B. 14 (2007) 77.

[32] A. Kumar, B. Prasad, I.M. Mishra, J. Hazard. Mater.152 (2008) 589.

[33] D.H. Lataye, I.M. Mishra, I.D. Mall, Ind. Eng. Chem. Res. 45 (2006) 3934.

[34] J. Laine, S. Yunes, Carbon 30 (1992) 601.

[35] C.A. Toles, W.E. Marshall, M.M. Johns, Carbon 35 (1997) 1407.

[36] F. Suárez-García, A. Martínez-Alonso, J.M.D. Tascón, Carbon 39 (2001) 1111.

[37] R.A. Meyers, in: Encyclopedia of Analytical Chemistry, John Wiley & Sons Ltd., Chichester, 2000.

[38] H.A. Dabbagh, M. Yalfani, B.H. Davis, J. Mol. Catal. A: Chem. 238 (2005) 72.

[39] V. Sricharoenchaikul, C. Pechyen, D. Aht-ong, D. Atong, Energy & Fuels 22 (2008) 31.

[40] D.A. Skoog, F.J. Holler, S.R. Crouch, in: Principles of Instrumental Analysis, 6th ed., Thomson Brooks/Cole Publishing, Belmont, CA, 2007.

[41] M.K. Aroua, S.P.P. Leong, L.Y. Teo, C.Y. Yin, W.M.A.W. Daud, Bioresour. Technol. 99 (2008) 5786.

[42] B.M. Babic, S.K. Milonjic, M.J. Polovina, B.V. Kaludierovic, Carbon 37 (1999) 477.

[43] I. Langmuir, J. Am. Chem. Soc. 40 (1918) 1361.

[44] H.M.F. Freundlich, Z. Phys. Chem. 57 (1906) 385.

[45] K. Kadirvelu, C. Namasivayam, Environ. Technol. 21 (2000) 1091.

[46] T.W. Webi, R.K. Chakravort, AIChE 20 (1974) 228.

[47] M. Imamoglu, O. Tekir, Desalination 228 (2008) 108.

[48] V.K. Gupta, I. Ali, J. Colloid Interface Sci. 271 (2004) 321.

[49] L.A. Teles de Vasconcelos, C.G. Gonzalez Beca, Eur. Water Pollut. Contr. 4 (1994) 41.

[50] J. Acharya, J.N. Sahu, C.R. Mohanty, B.C. Meikap, Chem. Eng. J. 149 (2009) 249.

[51] S. Lagergren, Handlingar 24 (1898) 1.

[52] K.G. Bhattacharyya, A. Sharma, J. Hazard. Mater. 113 (2004) 97.

[53] M. Ajmal, R.A.K. Rao, R. Ahmad, M.A. Khan, J. Hazard. Mater. 135 (2006) 242.

[54] M.N. Zafar, R. Nadeem, M.A. Hanif, J. Hazard. Mater. 143 (2007) 478.

[55] Y.S. Ho, G. Mckay, Process Biochem. 34 (1999) 451.

[56] W.J. Weber, J.C. Morris, in: Proc. Int. Conf. on Water Pollution Symp., Pergamon Press, Oxford, 1962.